ADDIS ABABA UNIVERSITY
ADDIS ABABA INSTITUTE OF TECHNOLOGY
CENTER OF BIOMEDICAL ENGINEERING

BRAIN TUMOR DETECTION BASED ON MAGNETIC RESONANCE IMAGE ANALYSIS

BY
AMARE AMBAW TEGEGNE

A thesis submitted in partial fulfillment of the requirements for the Degree of Master of Science in Biomedical Engineering (Bioinstrumentation and Imaging)

ADVISOR

DR. DAWIT ASSEFA HAILE

Addis Ababa, Ethiopia, January, 2018

Declaration

I, the undersigned, declare that this thesis is my original work. It has never been presented for a degree in any other institution and that all sources of materials used in it have been duly acknowledged.

Name: _____

Signature: _____

Date: _____

This MSc. thesis has been submitted for examination with my approval as an advisor.

_____

Dawit Assefa Haile (PhD.)

Addis Ababa University

School of Graduate Studies

Certificate of Examination

This is to certify that the thesis prepared by Amare Ambaw Tegegne entitled*: "B*rain tumor detection based on Magnetic Resonance Image Analysis" submitted in partial fulfillment of the requirements for the degree of Master of Science in Biomedical Engineering (Bioinstrumentation and Imaging) complies with the regulations of the University and meets the accepted standards with respect to originality and quality.

Signed by the examining committee

Examiner _____Signature _____Date_____

Examiner _____Signature _____Date_____

Examiner _____Signature _____Date_____

Advisor _____Signature _____ Date_____

_____

Chief of Department or Graduate program coordinator

Abstract

Automatic detection of brain tumors based on magnetic resonance (MR) image processing has been developed in this thesis. Improving the ability to accurately identify early-stage tumors is important goal for physicians, because early detection of brain tumors is a key factor in producing successful treatments. In this regard, an automatic brain tumor detection and segmentation framework has been proposed in this thesis work based on contrast enhanced T1 weighted (T1-W) images acquired from a cohort of patients with confirmed high grade brain tumors. Gray scale T1-W images have been represented in the three component Trinion space and Trinion Fourier transform has been applied aiming to extract useful features that could be used to automatically detect and segment brain tumors from their surrounding background. The performance of the proposed scheme has been evaluated by comparing its segmentation outputs with the ground truth information (based on manual contours by radiologists) that came with the MR data set. Results have showed that the algorithm achieved 99.6% sensitivity, 100% specificity, and 99.8% accuracy for pixel based segmentation while it achieved 91.5% sensitivity, 90% specificity and 90.5% accuracy for image based classification of tumors.

Acknowledgement

First of all, I would like to thank God who gives courage for my life.

I would like to thank my advisor Dr. Dawit Assefa Haile for his continuous support, encouragement and invaluable comments from initial proposal of this thesis research to the end.

My special thanks for all Biomedical Engineering staffs of the Addis Ababa Institute of Technology for providing such a conducive environment throughout my study.

I also would like to thank my friends and all my classmates for the time we had together.

Finally, I sincerely thank my parents for their constant love, support and encouragement.

Table of Contents

List of Figures

List of Tables

Acronyms

2D	Two Dimensional
ANN	Artificial Neural Network
BPNN	Back Propagation Neural Network
CBTRUS	Central Brain Tumor Registry of the United States
CJD	Creutzfeld- Jakob disease
CMYK	Cyan, Magenta, Yellow and Kay
CSF	Cerebrospinal Fluid
CT	Computed Tomography
FLAIR	Fluid Attenuated Inversion Recovery
FN	False Negative
FP	False Positive
FSE	Fast Spin Echo
GBM	Glioblastoma Multiforme
GLCM	Gray Level Co-occurrence Matrix
GM	Gray Matter
GTSDM	Grey-Tone Spatial Dependence Matrices
GUI	Graphical User Interface
HSL	Hue Saturation Luminance
MR	Magnetic Resonance
MRI	Magnetic Resonance Imaging
NEMA	National Electrical Manufacturers Association
PC	Personal Computer
PCA	Principal Component Analysis
PET	Positron Emission Tomography
QFT	Quaternion Fourier transform
RF	Radio Frequency
RGB	Red Green Blue
ROI	Region of Interest
SE	Spin Echo
SPECT	Single Photon Emission Computed Tomography
SVM	Support Vector Machine
T1-W	T1-Weighted
T2-W	T2-Weighted
TE	Echo Time
TFT	Trinion Fourier transform
TN	True Negatives
TP	True Positives
TR	Repetition time
TS	Trinion S Transform
UK	United Kingdom
WHO	World Health Organization
WM	White Matter

Chapter One

1. INTRODUCTION

1.1 Background

Brain tumor is a cluster of abnormal cells growing in the brain. There are two types of brain tumors: primary brain tumors and secondary (metastatic) brain tumors. Primary brain tumors are those that begin in the brain and tend to stay in the brain, and can be malignant (cancerous) or benign (noncancerous). Metastatic brain tumors begin as a cancer elsewhere in the body and migrate, or metastasize, to the brain, and they are malignant. There are more than 120 different types of brain tumors; some are malignant, many are benign. The cause of brain tumors is unknown. Benign or malignant, primary or metastatic, brain tumors are treatable.

Early and accurate diagnosis of brain tumors is the key for implementing successful therapy and treatment planning. In the recent past, several research works have been done for the diagnosis and treatment of brain tumors based on imaging with different modalities. However, the diagnosis is a very challenging task due to the large variance and complexity of tumor characterization in images, such as size, shape, location and intensities, and can only be performed by professional neuro-radiologists. In this regard, use of the non-invasive Magnetic Resonance Imaging (MRI) has been a tremendous help due to its flexibility, efficiency, and superior soft-tissue contrast compared to other imaging modalities such as computed tomography (CT).

The use of computer technology in medical decision support is now widespread and pervasive across a wide range of medical areas such as cancer research, gastroenterology, brain tumors etc. MRI is a viable option now for the study of tumors in soft tissues. The method is very helpful in finding tumor types, size and location. MR uses magnetic fields to build up a picture and has no known side effects related to radiation exposure. It has much higher details in soft tissues. Effective analysis of such images is not only important to accurately detect tumors but also in extracting biomarkers for cancer patient’s response quantification such as tumor progression and also survival.

Various researchers have proposed different features for use in characterizing tumors in MRI. Image intensity, symmetry, textures, patterns, and other statistical features which utilize gray values of tumors are often used for tumor characterization. However the gray values of MR images tend to change due to over–enhancement or in the presence of noise [1]. That means features like intensity, for example, for use in classifying tumors would have limited use. Hence a way of extracting more efficient features could be vital.

In image processing, feature extraction is a special form of dimensionality reduction. When the input data to an algorithm is too large to be processed and it is suspected to be notoriously redundant (much data, but not much information) then the input data will be transformed into a reduced set of features (also termed feature vector). Transforming the input data into the set of features is called feature extraction. If the features extracted are carefully chosen it is expected that the features set will extract the relevant information (brain cancer tissue in our case) from the input data in order to perform the desired task using this reduced representation instead of the full size input [2].

1.2 Statement of the Problem

Now-a-days, one of the main causes for increasing mortality among children and adults is brain tumor. It has been concluded from the researches done previously that the number of people suffering and dying from brain tumors has been increasing. According to the Central Brain Tumor Registry of the United States (CBTRUS), it was projected that 80,000 new cases of primary brain and central nervous system tumors diagnosed by the end of 2016 [3]. Overall, more than 700,000 people currently live with the disease in the US according to data published in January 2017 and the mortality rate is considered very high [4]. This high mortality rate of brain tumors greatly increases the importance of brain tumor detection. Real time diagnosis of tumors by using more reliable algorithms, thus, becomes the main focus of the latest developments in medical imaging and detection of brain tumors in MR and CT scanned images. Separation of tumor cells and their nuclei from the rest of the image content is one of the main problems faced by most of the medical imagery diagnosis systems. The process of separation, i.e. segmentation, has vital importance in the construction of a robust diagnosis system. Image segmentation performed on the input

images enables easier analysis of the images thereby leading to better tumor detection efficiency. Hence image segmentation is the fundamental task in tumor detection.

Several methods have been developed in the literature by many researchers for use in segmentation of brain tumors in MR images. In that regard, this thesis thoroughly reviews the applicability of the different schemes available in the literature and evaluates their merits and demerit and finally proposes a mathematical algorithm that is more effective and robust in segmenting brain tumors based on useful features extracted from brain MR images.

1.3 Thesis Objectives

1.3.1 General Objective

To develop a framework for accurate segmentation of a large class of brain tumors in single parameter MR images.

1.3.2 Specific Objectives

- To extract non redundant features from MR images.
- To detect and segment tumors from single parameters MR images.
- To classify tumorous and non-tumorous MR image slices.
- To compare segmentation performance with available gold standard.

1.4 Significance of the Study

The growing incidence of brain tumors increases the number of images that need to be reviewed by oncologists/radiologists. In addition, particularly in a low resource setting, the high cost of examinations and lack of trained experts hinder patients from receiving the service. In this regard, automating brain tumor detection could deliver many potential benefits. In a screening setting, it allows the examination of a large number of images objectively in less time than current observer driven techniques which are subjective. It can also be an important diagnostic aid and can reduce the workload of trained graders, thereby reducing costs inside clinics. The work in this thesis is comprised of robust image analysis algorithm development with potentially useful pre-clinical and clinical applications which could contribute a lot to the existing problems.

Reference

[1]. V. P. Gladis, P. Rathi, S. Palani, “Linear discriminant analysis for brain tumor classification using feature selection”, Int. J Communication and Engineering, 2010, Vol 5, Issue 4 , pp. 1179-1185.

[2]. M. Egmont –Petersen, D. de Ridder, “Image processing with neural networks- a Review”“, Pattern recognition, 2002, Vol 35, pp. 2279-2301.

[3]. http://www.abta.org/about-us/news/brain-tumor-statistics/, Accessed on January 1, 2015.

[4]. http://www.cbtrus.org/factsheet/factsheet.html, Accessed on January 23, 2015.

Chapter Two

2. HUMAN BRAIN AND BRAIN TUMOR

2.1 Medical Background

2.1.1 Brain Anatomy Overview

The human brain is a highly specialized organ. It serves as the control center for functions of the body, interprets information from outside world and embodies the essence of mind and soul. Intelligence, creativity, emotion, and memory are a few of many things governed by the brain [1]. In this section we describe the brain tissue structure and anatomical parts of the brain that we need to know for the purpose of this thesis.

Broadly speaking, the three brain tissue types are gray matter (GM), white matter (WM) and cerebrospinal fluid (CSF). GM is made of neuronal and glial cells, also known as neuroglia or glia, respectively, that control brain activity and the basal nuclei which are the gray matter nuclei located deep within the WM. The basal nuclei include: caudate nucleus, putamen, pallidum and claustrum. WM fibers are myelinated axons which connect the cerebral cortex with other brain regions. The corpus callosum, a thick band of white matter fibers, connects the left and right hemispheres of the brain. The CSF consists of glucose, salts, enzymes, and white blood cells. This fluid circulates through channels (ventricles) around the brain and the spinal cord to protect them from injury. There are also another tissues called meninges which are the membranes covering the brain and spinal cord [2]. An MR image with GM, WM and CSF components is illustrated in Figure 1 below.

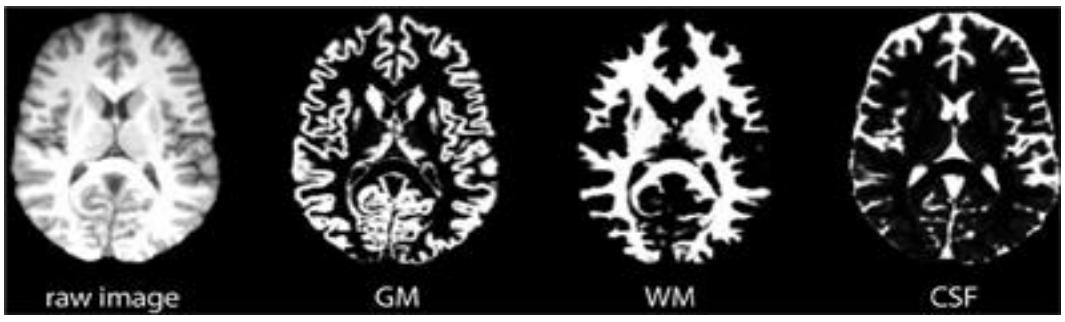

Figure 1: Illustration of Gray Matter (GM), White Matter (WM) and Cerebro Spinal Fluid (CSF).

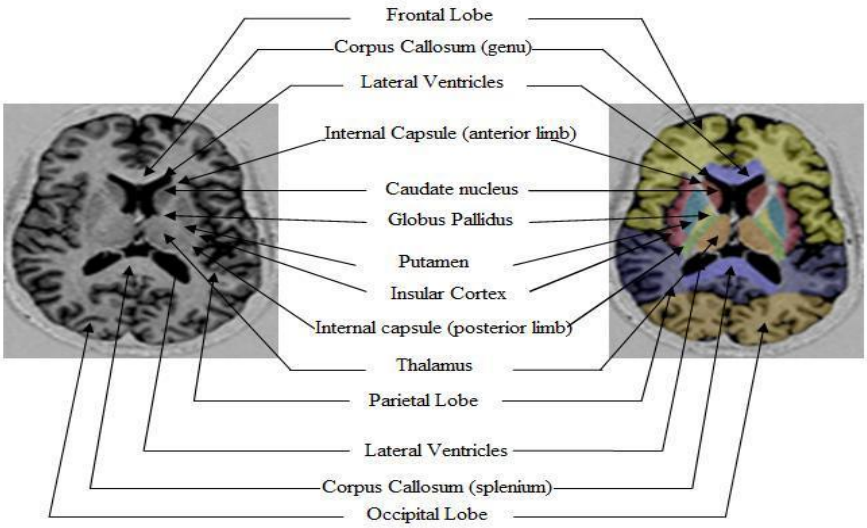

Figure 2: Overview structure of human brain: an axial slice MR image (left), the color coded version of the MR image on the left side (right) [3].

Anatomically the brain is composed of the cerebrum, the cerebellum and the brain stem as shown in Figure 2. The *cerebrum* is the largest part of the brain and composed of right and left hemispheres, each controlling the opposite side of the body, and it performs higher functions like interpreting touch, vision and hearing, as well as speech, reasoning, learning, and fine control of movement. Each hemisphere is divided into four lobes: the frontal, temporal, parietal, and occipital lobes. The *cerebellum* is the second largest structure of the brain and it coordinates muscle movements and maintains posture and balance. It is located at the back of the brain and is connected to brain stem. Both, cerebrum and cerebellum have a thin outer cortex of GM, internal WM and small, deeply situated masses of GM. The *brain stem* is located at the bottom of the brain and is connected to the spinal cord. It performs many automatic functions such as breathing, heart rate, body temperature, wake and sleep cycles, digestion, sneezing, coughing, vomiting, and swallowing. It has three structures: the midbrain, pons and medulla oblongata [2] (see Figure 3).

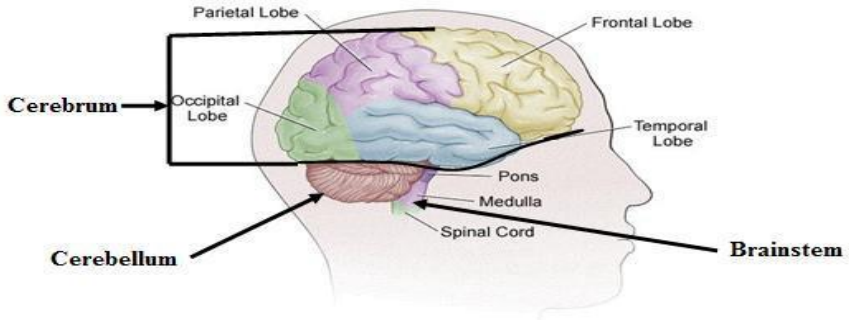

Figure 3: The major subdivisions of the human brain [3].

2.1.2 Brain Tumors

A brain tumor is an abnormal mass of tissue in which some cells grow and multiply uncontrollably, apparently unregulated by the mechanism that control normal cells. The growth of a tumor takes up space within the skull and interferes with normal brain activity. A tumor can cause damage by increasing pressure in the brain, by shifting the brain or pushing against the skull, and by invading and damaging nerves and healthy brain tissues [4].

Brain tumors are classified depending on the exact site of the tumor, the type of tissue involved, whether they are noncancerous (benign) or cancerous (malignant), site of origin (primary or secondary) and other factors [5]. According to the World Health Organization (WHO), there are more than 120 types of brain tumors. The WHO classifies brain tumors by cell origin and how the cells behave, from the least aggressive (benign) to the most aggressive (malignant).

According to Cancer Research UK, it is estimated that every year there are almost 445,000 news cases of brain tumours worldwide [6]. The most common brain tumors are gliomas, which begin in the glial tissue. According to some histology statistics, 50.3% of all brain tumors are gliomas (Glioblastoma 52%; Astrocytoma 26%; and Oligodendroglioma, Ependymoma, etc make up 22%), 20.9% are Meningiomas, 15% Pituitary while 8% are Acoustic Neuroma, Nerve Sheath Tumors and others combined, and the rests are unknown or unspecified tumors [6].

Secondary brain tumours, that are always malignant, are also known as metastatic cancers as they are the result of the spreading of other cancers that are growing somewhere else in the body. They are given the name of the origin cancer and these are the most common types of brain tumours (10 to 15% of cancer patients develop metastatic cancer to the brain). The derivations of these metastatic cancers percentage wise are: lung (35%), breast (20%), melanoma (10%), renal cell (10%), and colon (5%) [6].

2.2 MRI Brain Imaging and Characteristics of Brain Tumors

There are a variety of imaging techniques used to study brain tumors, such as: magnetic resonance imaging (MRI), computed tomography (CT), positron emission tomography (PET), single photon emission computed tomography (SPECT) imaging and cerebral

angiography. In recent years, CT and MR imaging are the most widely used techniques, because of their widespread use and their ability to produce high resolution images of normal anatomic structures and pathological tissues. MRI is a method used to visualize pathological or other physiological alterations of living tissues and is commonly used for brain tumor imaging because of the following reasons [7]:

- It does not use ionizing radiation like CT, SPECT and PET;
- Its contrast resolution is higher than other techniques mentioned above;
- Ability of MRI devices to generate 3D space images enables them to have superior tumor localization, and
- Its ability in acquisition of both functional and anatomical information about the tumor during the same scan.

Before discussing the MR image characteristics of brain tumors, it is important to describe its working principle. During MR imaging, the patient is placed in a strong magnetic field which causes the protons in the water molecule of the body to align in either parallel (low energy) or anti-parallel (high energy) orientation with the magnetic field. Then a radiofrequency (RF) pulse is introduced which forces the spinning protons to move out of equilibrium state. When the RF pulse is stopped, the protons return to equilibrium state and produce a sinusoidal signal at a frequency dependent on the local magnetic field. Finally, the RF coil or resonator within the scanner detects the signal and creates the image [8].

When the resonator detects a signal under controlled condition, different images can be acquired and information related to tissue contrast may be obtained, revealing details that can be missed in other conditions. The amount of signal produced by specific tissue types is determined by the number of mobile hydrogen protons, the speed at which they are moving, and the time needed for the protons within the tissue to return to their original state of magnetization (T1 relaxation time) and the time required for the protons perturbed into coherent oscillation by the RF pulse to lose their coherence (T2 relaxation times). As T1 (spin-lattice) and T2 (spin-spin) relaxation times are time dependent, the timing of the RF pulse and the reading of the radiated RF energy change the appearance of the image. The repetition time (TR) describes the time between successive applications of RF pulse sequences. The echo time (TE) describes the delay

before the RF energy radiated by the tissue in question is measured. The pulse sequence, which is described by the TR and TE indicates the technique used to administer the RF energy, can be chosen to maximize the effect of differences in T1 or T2. This gives rise to the description of MR images as T1, T2 and proton density (ρ) weighted images. The T1-W images (short TR and short TE) provide better anatomical detail and, if used with contrast enhancement can provide anatomical and pathological details. The T2-W images (long TR and long TE) are sensitive to pathology. ρ weighted images (long TR and short TE), where number of protons per unit volume in tissues is the main factor in determining formation of image contrast, shows anatomy and some pathology [8,9,10].

There are two main MR imaging sequence families, depending on the type of echo recorded: spin echo (SE) sequence and gradient echo (GE) sequences. SE sequence with its variant fast spin echo (FSE) sequence has been the standard MRI pulse sequences for anatomical and pathological details [9]. SE is when we irradiate a sample with two or more RF pulses and observe an echo signal that has its peak energy at some time after the RF pulses and GE is, on the other hand, an echo signal that is intentionally generated by application of a rephasing gradient pulse to counter a previous dephasing gradient pulse on the same physical axis [11].

Brain images in MRI scan can be normal or abnormal. As mentioned in the beginning of the current chapter, the normal brain is characterized by having GM, WM and CSF tissues. The abnormal brain usually contains active tumor, necrosis and edema in addition to the normal brain tissues. Necrosis is a dead cell located inside an active tumor, while edema is located near active tumor borders. Edemas, which result from local disruption of blood brain barrier, often overlap with normal tissues and it is always difficult to distinguish [12].

The intensity values seen on an MRI scan for a particular brain depend primarily on the content of that pixel versus neighboring tissue and on other factors including the presence of abnormality. In normal brain MR images, intensity level of brain tissues in the order of increasing brightness is CSF, GM, and WM in T1-W image, as illustrated in Figure 4 (see also Figure 1 in the previous section).

In tumorous brain MR images intensity level of tumorous tissues exhibit different intensity level on T1-W and T2-W images based on the type of tumor. On T1-W most

tumors have low or intermediate signal intensity but for some tumors this does not hold true. For example, Glioblastoma multiforme (GBM), the highest grade (grade 4) glioma tumor, has high signal intensity. On T2-W most tumors have bright intensity but there are tumors which have low intensity, the classic examples are lymphoma tumors [12].

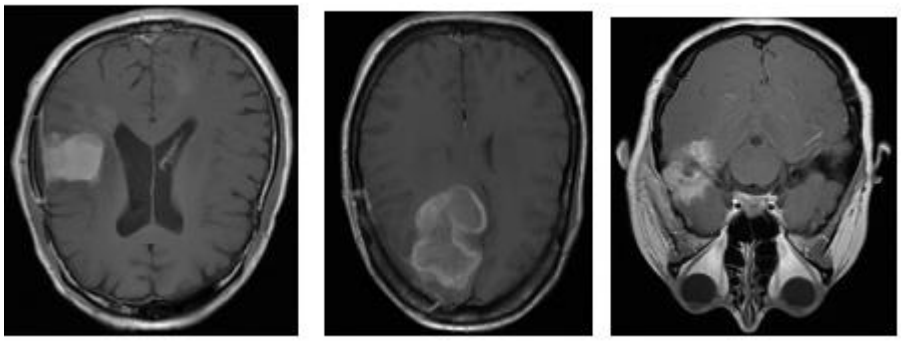

Figure 4: Typical Glioblastoma multiforme (grade 4 glioma) brain tumor axial T1-W contrast enhanced MRI scans.

Data used in this thesis for the purpose of detecting and segmenting glioma tumors are axial T1-W contrast enhanced brain MRI scans of patients with confirmed GBM.

Reference

[1]. www.mayfield.com, Accessed on January 23, 2016

[2]. Charles R. Noback, Norman L. Strominger, Robert J. Demarest and David A. Ruggiero, The Human Nervous System: Structure and Function, 6th ed., Humana Press, 2005.

[3]. http://www.teamrads.com/Cases/Neuroanatomy/MRI, Accessed: June 12, 2014.

[4]. Louis D. N., Ohgaki H., Wiestler O. D, Cavenee W. K. (Eds.), WHO Classification of Tumors of the Central Nervous System, International Agency for Research on Cancer (IARC), Lyon, France, 2007.

[5]. Jan C. Buckner, et al., Central Nervous System Tumors, Mayo Clinic Proceedings, Vol. 82, No. 10, 2007, pp. 1271-1286.

[6]. Cancer Research UK, Brain, other CNS and intracranial tumours incidence statistics, 28 March 2013. [Online] Available: http://www.cancerresearchuk.org/cancer-info/cancerstats/types/brain/incidence/#Distribution. [Accessed: 17 April 2015].

[7]. Medical Imaging in Cancer Care: Charting The Progress, US Oncology and National Electrical Manufacturers Association (NEMA), Accessed January 20, 2015 at http://www.healthcare.philips.com/pwc_hc/us_en/about/Reimbursement/assets/docs/cancer_white_paper.pdf

[8]. A. O Rodriguez, Principles of Magnetic Resonance Imaging, Revista Mexicana de Fisica, Vol. 50, No. 3, 2004, pp. 272-286.

[9]. Joseph P. Hornark, The Basics of MRI, Accessed: January 12, 2012, at http://www.cis.rit.edu/htbooks/mri/

[10]. Catherine Westbrook, MRI at Glance, Blackwell Science Publishing, 2002.

[11]. http://www.radiologyassistant.nl/, Accessed: June, 14, 2015.

[12]. J.P. Hornak, The Basics of MRI, online at http://www.cis.rit.edu/htbooks/mri/ [Accessed 17 Sept 2017].

Chapter Three

3. ELEMENTS OF COMPUTER-AIDED DETECTION

3.1 Introduction

This chapter presents and discusses the background literature on computer based processing paradigms of brain tumor detection. Section 3.2 presents the fundamental concepts of digital image processing with emphasis on image segmentation techniques used in brain tumor detection applications. Section 3.3 gives highlights on existing automatic brain tumor detection techniques available in the literature.

3.1.1 MRI Based Computer-Aided Detection Systems

In recent years, major effort has been made to develop MRI applications which can assist radiologists in the detection and characterization of malignant and benign abnormalities. Computer-aided systems identify and mark suspicious regions on MR images to bring them to the attention of radiologists. These systems minimize search, perception and interpretation errors even if radiologists fail to recognize suspicious abnormalities. The visual assessment by the radiologists, which is subjective and showing observer variability, could be very time consuming and often non repetitive; computer-aided systems then come to the rescue. The following section provides the fundamental of digital image processing.

3.2 Fundamentals of Digital Image Processing

The knowledge of the concepts of digital image processing presented in the following sections is required to fully comprehend the methods discussed in this thesis. In particular, emphasis is given on the image processing and segmentation techniques, which have been reported in the literature as reviewed in Section 3.3. Image processing considers the image for a specific application and it is useful in many applications such as computer vision, medical imaging, and pattern recognition. It extracts the useful information from the image. Image processing mainly involves

image segmentation, image transformation, pattern classification, and feature extraction [1].

3.2.1 Representation of a Digital Image

An image (gray-scale or monochromatic image) is defined as a two dimensional (2D) function, *f(x, y)*, where *x* and *y* are spatial coordinates, and *f(x, y)* is a set of grey-tones. When *x, y* and the grey-tones of *f* are discrete quantities, the image is called a digital image [1]. A discrete image of size N_x X N_y can be represented as a 2D matrix as:

$$f(x,y) = \begin{bmatrix} f(0,0) & f(0,1) & \dots & f(0,N_y-1) \\ f(1,0) & f(1,1) & \dots & f(1,N_y-1) \\ \vdots & & \vdots & \vdots \\ f(N_x-1,0) & f(N_x-1,1) & \dots & f(N_x-1,N_y-1) \end{bmatrix}$$

A digital image has a finite number of elements; each of these elements has a particular value and location. These elements are called pixels or image elements [1].

Digital images may come in different types; some of these are the following [2].

- Binary image: This is the simplest type of image with two gray-values, 0 and 1 or black and white. Each pixel is represented by a single bit. These types of images are useful in computer vision applications where only information about images or outlines are required. It can be created from a gray-scale image that uses 0 for pixels with gray levels below a threshold and 1 for other pixels but this way of creation of a binary image is often problematic as most of the information of the original gray-scale image is lost.

- Gray-scale image: These images contain brightness information. The number of bits that are used to represent each pixel are related to the number of different brightness levels available. A typical gray-scale image contains 8 bits per pixel so there are 256 different possible gray-tones/intensity values ranging from 0 to 255.

- Color image: Normally, images are represented as RGB (Red, Green, and Blue) models, and each color pixel has 24 bits (8 bits per color component). The brightness information and color information are coupled and could be represented in different color spaces such as HSV, Lab, CMYK and the like.

A digital image can be presented in different ways. It can be plotted as a surface with three dimensions *(x, y, z)*, in which *x, y* are spatial coordinates, and *z* is the value of *f(x, y)*. The same image could also be presented as a visual intensity array. Another method is to represent the image as a 2D array. This is useful particularly when the size of the image is big and only part of it needs to be analyzed.

3.2.2 Feature Extraction

Feature extraction is a method of capturing visual content of an image. It is the process to represent a raw image in its reduced form to facilitate decision making such as pattern classification. In image processing, feature extraction is a special form of dimensionality reduction. When the input data to an algorithm is too large to be processed and it is suspected to be notoriously redundant (much data, but not much information), then the input data will be transformed into a reduced set of features (also named features vector). Transforming the input data into the set of features is what we call feature extraction. If the features extracted are carefully chosen, it is expected that the features set will extract the relevant information from the input data in order to perform the desired task using this reduced representation instead of the full size input.

Features, the characteristics of the objects of interest, if selected carefully are representatives of the maximum relevant information that the image has to offer for a complete characterization of an object of interest. Feature extraction methodologies analyze objects and images to extract the most prominent features that are representative of the various classes of the objects/images. Features are used as inputs to classifiers that assign them to the class that they represent. In this context, the purpose of feature extraction is to reduce the original data by measuring certain properties, or features, that distinguish one input pattern from another pattern. The extracted feature should provide the characteristics of the input type to the classifier by considering the description of the relevant properties of the image into feature vectors. Features are divided into different classes based on the kind of properties they describe. Some important features are described below.

Color: From a mathematical viewpoint, the color signal is an extension from scalar-signals to vector-signals. The color can be represented by an average color (three scalars) or a color histogram (three functions). Color features can be derived from a

histogram of the image. The multi-dimensional histogram is used for the multi-color image [3]. From a brightness histogram, the color features are derived as RGB components. Color features are useful for biomedical image processing, such as for cell classification, and cancer cell detection [3]. One weakness is that the color histograms of two different scenes/objects having the same color are similar limiting the application of color histograms in object classification and recognition. In that regard there are other color manipulation techniques reported in the literature with better capability than color histograms.

Texture: There is no unique definition for texture. Texture is a characteristic of an image that can provide a higher-order description of the image and includes information about the spatial distribution of tonal variations or gray tones [4]. An image can have one or more textures. These features are useful in many applications such as in medical imaging [5], remote sensing [6], and content based image retrieval.

Structure: This feature describes the structure of the image or the locations of objects in the image in contrast to each other. For example, an image may include different objects such as trees, a bird, a cat etc.

Shape: From the human point of view, shape is a high-level concept but mathematically shape is a low-level element. In pattern recognition, shape is described as a function of position and direction simply as a connected curve within a 2D field [7]. Shape features can be used for medical applications for example for cervical cell classification or for content-based image retrieval systems where color features are not useful [8].

3.2.3 Texture Analysis

Texture analysis refers to the branch of imaging science that is concerned with the description of characteristic image properties by textural features. However, there is no universally agreed-upon definition of what image texture is and in general different researchers use different definitions depending on the particular area of application [9]. Texture can be defined as the spatial variation of pixel intensities, which is a definition that is widely used and accepted in the field. The main image processing disciplines in which texture analysis techniques are used are classification, segmentation and synthesis. In image classification the goal is to classify different

images or image regions into distinct groups [10]. Texture analysis methods are well suited to this because they provide unique information on the texture, or spatial variation of pixels, of the region where they are applied. In image segmentation problems, the aim is to establish boundaries between different image regions [11]. By applying texture analysis methods to an image, and determining the precise location where texture feature values change significantly, boundaries between regions can be established. Synthesizing image texture is, for example, important in three-dimensional (3D) computer graphics applications where the goal is to generate highly complex and realistic looking surfaces.

There are two main approaches often used to analyze image textures:

1. Structural approach: here texture is defined to be a set of primitive texels (texture elements) in some regular or repeated relationship [12].
2. Statistical approach: in this case texture is defined as a quantitative measure of the arrangement of intensities in a region [12].

While the first approach is appealing and can work well for man-made, regular patterns, the second approach is more general and easier to compute and is used more often in practice [12].

Statistical Approaches for Texture Analysis

To examine an image using texture analysis, the image is treated as a textured surface. This is illustrated in Figure 5 which shows the textured intensity surface representation of a 2D medical image. In first-order statistical texture analysis, information on texture is extracted commonly from the histogram of the image intensity. This approach measures the frequency of a particular grey-level at a random image position and does not take into account correlations, or co-occurrences, between pixels. In second-order statistical texture analysis, information on texture is based on the probability of finding a pair of grey-levels at random distances and orientations over an entire image. Extension to higher-order statistics involves increasing the number of variables studied.

Many conventional approaches used in the literature to study texture have concentrated on using 2D techniques to compute features relating to image texture. This approach has been used extensively to describe different image textures by unique features and has found applications in many disparate fields. Such method has been used for example for discrimination of terrain from aerial photographs [13], for

in-vitro classification of tissues from intravascular ultrasound [14] and for identification of prion protein distribution in cases of Creutzfeld-Jakob disease (CJD) [15]. Other applications include classification of pulmonary emphysema from lung based on high-resolution CT images [16-18] and identification of normal and cancerous pathology [19-21]. Higher-order approaches have been used, for example, to localize thrombotic tissue in the aorta [22] and to determine if functional vascular information found in dynamic MR sequences exists on anatomical MR sequences [23]. Extension of these approaches to 3D is continuing to develop within the machine vision community.

Several authors have reported the application of 2D texture analysis methods on a slice-by-slice basis through volumetric data, however, it has been reported that with this approach information may be lost [24, 25]. Findings reported by Xu et al., on the use of 3D textural features for discriminating between smoking related lung pathology, demonstrate the power of this approach for this particular application [24]. In another study, Kovalev et al. showed that an extended 3D co-occurrence matrix approach can be used for the classification and segmentation of diffuse brain lesions on MR image data [24]. However, the slice based approach is still in use by many researchers.

Texture analysis has also been used to identify unique pathology on multi-modality images of cancer patients. Using the local binary operator to analyze the weak underlying textures found in transrectal ultrasound images of the prostate, Kachouie and Fieguth demonstrated that the approach was suitable for segmentation of the prostate [26]. In another cancer-related study of 48 normal images and 58 cancer images of the colon, Esgiar et al. demonstrated that by adding a fractal feature to traditional statistical features the sensitivity of the classification improved [27].

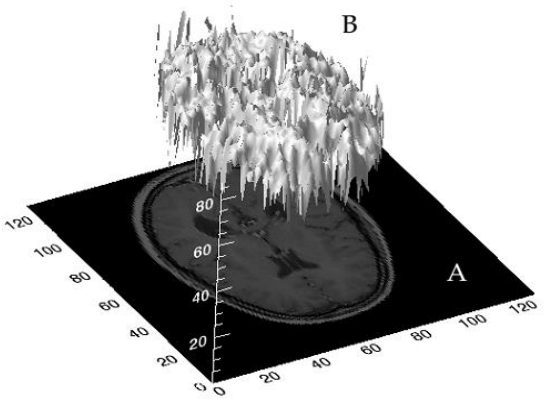

Figure 5: 3D textured intensity surface representation of a medical image. (A): 2D MR image of brain and (B): Pixel values of the MR image plotted on the vertical axis to produce a 3D textured surface.

First-Order Statistical Texture Analysis

First-order texture analysis measures use the image histogram or pixel occurrence probability to calculate texture. The main advantage of this approach is its simplicity through the use of standard descriptors (e.g. mean and variance) to characterize the data [28]. However, the power of the approach for discriminating between unique textures is limited in certain applications because the method does not consider the spatial relationship, and correlation, between pixels. For any surface, or image, grey-levels are in the range $0 \leq i \leq N_g - 1$, where N_g is the total number of distinct grey-levels. If $N(i)$ is the number of pixels with intensity i and M is the total number of pixels in an image, it follows that the histogram, or pixel occurrence probability, is given by,

$$\boldsymbol{P(i)} = \frac{\boldsymbol{N(i)}}{\boldsymbol{M}} \tag{1}$$

First order features commonly used to describe the properties of the image histogram (and therefore image texture) include: mean, variance, coarseness, skewness, kurtosis, first order energy, and entropy.

Second-Order Statistical Texture Analysis

The human visual system cannot discriminate between texture pairs with matching second order statistics [29]. The first machine-vision framework for calculating second-order or pixel co-occurrence texture information was developed for analyzing aerial photography images [4]. In this technique, pixel co-occurrence matrices, which are commonly referred to as grey-tone spatial dependence matrices (GTSDM), are computed. The entries in a GTSDM are the probability of finding a pixel with grey-level i at a distance d and angle α from a pixel with a grey-level j. An essential component of this framework is that each pixel has eight nearest-neighbors connected to it, except at the periphery. As a result, four GTSDMs are required to describe the texture content in the horizontal ($P_H = 0^0$), vertical ($P_V = 90^0$), right- diagonal ($P_{RD} = 45^0$) and left-diagonal ($P_{LD} = 135^0$) directions. This is illustrated in Figure 6.

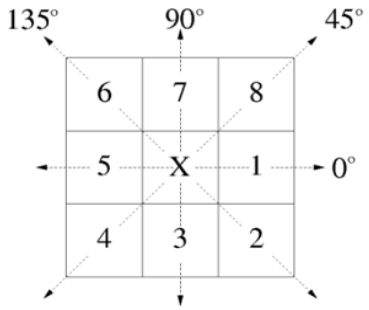

Figure 6: Eight nearest-neighbor pixels used in GTSDM framework to describe pixel connectivity. Cells 1and 5 show the horizontal (P_H), 4 and 8 the right-diagonal (P_{RD}), 3 and 7 the vertical (P_V) and 2 and 6 the left-diagonal (P_{LD}) nearest-neighbors.

An example of the calculation of a horizontal co-occurrence matrix (P_H) on a 4× 4 image containing four unique grey-levels is shown in Figure 7. A complete representation of image texture is contained in the co-occurrence matrices calculated in the four directions. Extracting information from these matrices using textural features, which are sensitive to specific elements of texture, provides unique information on the structure of the texture being investigated. Haralick et al., proposed a set of 14 local features specifically designed for this purpose [4]. In practice the information provided by certain features may be highly correlated or of limited practical use. A feature selection strategy is therefore useful with this approach to take account of redundant, or irrelevant, information. It is also interesting to note that prior to any processing, the GTSDMs, which are symmetric, can provide some useful information on the characteristics of the image being studied. For example, the co-occurrence matrix entries for a coarse texture will be heavily focused along the diagonals relative to the distance *d* between the pixels studied.

0	2	2	2
0	3	2	2
1	2	2	2
3	0	3	0

(P_H)

Grey-Level	0^0	0	1	2	3
	0	0	0	1	4
	1	0	0	1	0
	2	1	1	10	1
	3	4	0	1	0

Figure 7: Simple example demonstrating the formation of co-occurrence matrix from an image: 4x4 image with four unique gray-level (left) and the resulting horizontal co-occurrence matrix (P_H) (right).

3.2.4 Image Segmentation and Classification

There are three primary issues in texture analysis: classification, segmentation and shape recovery from texture. Image segmentation is a classification problem and therefore is one of the most important and difficult tasks in image processing. Classically, image segmentation is defined as the process of partitioning an image into mutually exclusive regions based on pixel characteristics. The goal of image segmentation is to assign each pixel to a group or class with similar characteristics. Ideally, classes with similar characteristics correspond to similar objects in an image [30]. For example, one of the aims of segmentation when analyzing MR images of the brain having a tumor is to obtain region of interest (ROI) containing all tumorous regions from the brain tissue.

Image segmentation approaches commonly discussed in the literature include: tresholding, region growing, classifier based, clustering, Markov random fields, artificial neural network, deformable models, and atlas-guided approaches, to mention a few. Detailed discussion on such segmentation approaches particularly those for use in medical images is available in ref. [31].

For example, in the case of brain tissue classification based on MR imaging, the patterns of brain tissues are classified as either normal or tumorous on the basis of the optimum subset texture features selected for machine learning modeling. A classifier trained on known MR image (ground truth MR image) combines the selected features and uses confidence measures to indicate that image is either normal or tumorous [32,33].

In this thesis a new classification scheme is developed for use in effective detection and segmentation of brain tumors based of useful features extracted from MR scans of patients with confirmed brain tumors. The next chapter explains details of the methodology developed and the back ground mathematics.

3.3 Review of Automatic Brain Tumor Detection Techniques

The goal of automatic detection of brain tumors from brain MR images is to identify the presence of abnormalities such as detecting the tumor and perform classification. Brain tumor detection is possible from a single parameter MR image (T1-W, T2-W, etc), or a combination of multiple MR parameters. Whichever way they are detected,

tumors need to be classified into their malignant and benign types; a technique many authors have tried to automate.

R. R. Laddha and S. A. Ladhake [34] proposed an algorithm for tumor detection based on segmentation and morphological operators. Firstly quality of the given MR scanned image is enhanced and then morphological operators are applied to detect the tumor in the scanned image. The authors additionally proposed a wavelet based algorithm for tumor detection which utilizes the complementary and redundant information from CT and MR images. The algorithm efficaciously utilizes the information provided by the CT and MRI images there by providing a resultant fused image which increases the efficiency of tumor detection.

K. Verma et al. [35] suggested a method that gives establishment of division and edge recognition. The work assessed current segmentation methodologies with an accentuation put on uncovering the points of interest and weaknesses of these routines for therapeutic imaging applications. The utilization of picture division in diverse imaging modalities is likewise portrayed alongside the troubles experienced in every methodology.

In another study, Ed-Edily Mohd. Azhari et al. [36] proposed a methodology comprised of five stages: picture capturing, pre-handling, edge identification, histogram bunching and morphological operations. After morphological operations, tumors show up as immaculate white shading on unadulterated dark foundations. The proposed tumor recognition and confinement framework was observed to have the capacity to precisely distinguish and limit cerebrum tumor in attractive reverberation imaging. The preliminary results showed how a straightforward machine learning classifier with an arrangement of basic picture based elements can bring about high grouping exactness. The results additionally showed the adequacy and proficiency of the five-stage mind tumor location and confinement approach persuading to extend the system to distinguish and limit an assortment of different sorts of tumors in different sorts of medicinal symbolism.

Another investigation by A. Laxami et al., [37] proposed a method for tumor segmentation aiming to improve computational issues. The study proposed significant feature points based approach for primary brain tumor segmentation. Axial slices of T1-W brain MR images with contrast enhancement were analyzed. In order to extract

significant feature points in the image, the authors applied a feature point extraction algorithm based on a fusion of edge maps using morphological and wavelet methods. Geometric transformations and image scaling were then applied followed by region growing algorithm to isolate tumor regions. Preliminary results showed that the approach achieved good segmentation results with reduced computational time.

In another study, K. K. Hiran and R. Doshi [38] proposed an Artificial Neural Network (ANN) approach for brain tumor detection. The work showed that the technique can effectively distinguish cerebral tumors and accordingly offer specialists for examining tumor sizes. P. S. Kumar and P. G. Kumar [39] in their study also proposed another approach to automated detection of brain tumor. The proposed work consisted of various stages in their diagnosis processing such as preprocessing, anisotropic diffusion, feature extraction and classification. Local binary patterns and gray level co-occurrence features, gray level and wavelet features were extracted and these features were trained and classified using Support Vector Machine (SVM) classifier. The achieved results were quantitatively evaluated and compared with various ground truth images. The proposed method offered fast and better segmentation and classification rate by yielding 99.4% of sensitivity, 99.6% of specificity, 97.03% positive predictive value and 99.5% of overall accuracy.

In another study, O. N. Pandey et al. [40] developed a technique for detection and extraction of cerebrum tumor from MR pictures. In this work, a strategy for division of brain tumor was developed based on division and morphological operators. The intent of the work was to outline a computerized apparatus for cerebrum tumor measurement utilizing MRI picture information sets.

The method proposed by P. John [41] for use in identification and characterization of brain tumors based on MR images utilized three major stages: (1) wavelet deterioration, (2) textural highlight extraction and (3) order. Discrete Wavelet Transform was initially utilized based on Daubechies wavelet, for breaking down the MR picture into diverse levels of inexact and point by point coefficients and afterward the dim level co-event network is framed, from which the surface measurements, for example, vitality, contrast, relationship, homogeneity and entropy are computed. The after effects of co-event grids are then encouraged into a probabilistic neural system for further arrangement and tumor identification. The proposed system has been connected on

genuine MR images, and the precision of arrangement utilizing probabilistic neural system is observed to be about 100%.

Magdi et al. [42] used an intelligent model for automatic brain tumor diagnosis based on MR images in which the (MR) images were classified into normal, edema, cancerous or neutral (not classified). The proposed method consisted of three stages. In the first stage preprocessing step was applied to remove noise and to enhance image contrast. Secondly texture features were extracted and then principal component analysis (PCA) was applied for dimension reduction. Finally Back-Propagation Neural Network (BPNN) based-on Pearson correlation coefficient was used to classify the brain images. The experimental results showed that the proposed model achieves accuracy of 96.8%.

D. Assefa et al. [43] have proposed a method to do effective brain tumor detection based on holistic analysis of multi-parametric MR images. The multiple MR parameters were combined as one entity and analyzed holistically using higher order Fourier transforms. Their approach was implemented in terms of classifying structures in MR images taken from a cohort of patients treated for glioblastoma multiforme (GBM), the highest grade and most aggressive of the gliomas. Their results showed that, as opposed to a serial analysis, a holistic use of the inter correlation information embedded among individual MR parameters may be vital in detecting objects of interest that are not readily available.

Reference

[1]. R. C. Gonzalez and R. E. Woods, Digital Image Processing, 3rd ed., Prentice Hall, 2007.

[2]. S. E. Umbaugh, Computer Imaging: Digital Image Analysis and Processing, Taylor and Francic Group, 2005.

[3]. N. G. Nguyen, R. S. Poulsen, and C. Louis, “Some New Color Features and Their Application to Cervical Cell Classifacation", Pattern Recognition 16 (1983), No. 4, 401-411.

[4]. R. M. Haralick, K. Shanmugam, and I. Denstien, “Textural Features for Image Classification", IEEE Transactions on Systems, Man and Cybernetics SMC-3 (1973), No. 6, 610-621.

[5]. M. A. Tahir, A. Bouridane, and F. Kurugollu, “An FPGA Based Coprocessor for GLCM and Haralick Texture Features and their Application in Prostate Cancer Classification”, Analog Integrated Circuits and Signal Processing 43 (2005), 205-215.

[6]. M. Schroder, M. Schrder, and A. Dimai, “Texture Information in Remote Sensing Images: A Case Study”, Workshop on Texture Analysis, 1998.

[7]. S. Brandt, “Use of Shape Features in Content-Based Image Retrieval”, Master Dissertation, Helesinki University of Technology, August 1999.

[8]. S. Brandt, J. Laaksonen, and E. Oja, “Statistical Shape Features in Content-Based Image Retrieval”, The 15th Int. Conf. on Pattern Recognition 2 (2000), 1062-1065.

[9]. Tuceryan, M. and Jain, A.K. (1998). Texture analysis. In: Chen, C.H; Pau, L.F. & Wang, P.S.P., (eds). *The handbook of pattern recognition and computer vision*. 2nd ed. World Scientific Publishing Co., ISBN 9-810-23071-0, Singapore.

[10]. Pietikainen, M.K. (ed) (2000). *Texture analysis in machine vision*, World Scientific Publishing, 981-02-4373-1, Singapore.

[11]. Mirmehdi, M.; Xie, X. and Suri, J. (eds) (2008). *Handbook of texture analysis,* Imperial College Press, 1-84816-115-8, UK.

[12]. Shapiro and Stockman,” Computer Vision”, Prentice Hall, March 2000.

[13]. Conners, R. and Harlow, C. , "Theoretical comparison of texture algorithms", *IEEE Transactions on Pattern Analysis and Machine Intelligence*, Vol. 2, No. 3, pp. 204-222, 1980.

[14]. Nailon, W. H., "*Tissue characterisation of intravascular ultrasound using texture analysis",* Ph.D. dissertation, The University of Edinburgh, School of Engineering, 1997.

[15]. Nailon, W.H. and Ironside, J.W., "Variant Creutzfeldt-Jakob disease: immunocytochemical studies and image analysis", *Microscopy Research & Technique*, Vol. 50, No. 1, pp. 2-9, 2000.

[16]. Uppaluri, R., Mitsa, T., Sonka, M., Hoffman, E. and McLennan G., "Quantification of pulmonary emphysema from lung computed tomography images", *American Journal of Respiratory Care in Medicine*, Vol. 156, No. 1, pp. 248-254, 1997.

[17]. Xu, D., Kurani, A. and Raicu, D., "Run-length encoding for volumetric texture", *Proceedings of 4th IASTED International Conference on Visualization, Imaging and Image Processing – VIIP*, Marbella, Spain, September 6th – 8th, 2004.

[18]. Xu, Y., Sonka, G., McLennan, G., Junfeng, G. and Hoffman, E., "MDCT-based 3D texture classification of emphysema and early smoking related pathologies", *IEEE Transactions on Medical Imaging*, Vol. 25, No. 4, pp. 464-475, 2006.

[19]. Karahaliou, A., Boniatis, I, Skiadopoulos, S. and Sakellaropoulos, F, "Breast cancer diagnosis: analyzing texture of tissue surrounding microcalcifications", *IEEE Transactions on Information Technology in Biomedicine*, Vol. 12, No. 6, pp. 731-738, 2008.

[20]. Zhou, B., Xuan, J., Zhao, H., Chepko, M., Freedman, M. and Yingyin, K., "Polarization imaging for breast cancer diagnosis using texture analysis and SVM", Proceedings of Life Sciences Systems and Applications Workshop, pp. 217-220, Bethesda, Maryland, USA, 2007.

[21]. Yu, H., Caldwell, C., Mah, K. and Mozeg D., "Co-registered FDG PET/CT based textural characterization of head and neck cancer in radiation treatment planning", *IEEE Transactions on Medical Imaging*, Vol. 28, No. 3, pp. 374-383, 2009.

[22]. Podda, B., Zanetti, G. and Giachetti, A, "Texture analysis for vascular segmentation from CT images", *Proceedings of Computer Assisted Radiology and Surgery (CARS)*, pp. 206-211, Berlin, Germany, 22nd-25th June, 2005.

[23]. Winzenrieth, R. and Claude, I., "Is there functional vascular information in anatomical MR sequences? A preliminary in vivo study", *IEEE Transactions on Biomedical Engineering*, Vol. 53, No. 6, June 2006, pp.1190-1194.

[24]. Kovalev, V., Kruggel, F., Gertz, H. and von Cramon D., "Three-dimensional texture analysis of MRI brain datasets", *IEEE Transactions on Medical Imaging*, Vol. 20, No. 5, pp. 424-433, 2001.

[25]. Kurani, A., Xu, D., Furst, J. and Raicu, D., "Co-occurrence matrices for volumetric data", *Proceedings of 7th IASTED International Conference on Computer Graphics and Imaging*, Kauai, Hawaii, USA, August 17 – 19, 2004.

[26]. Kachouie, N. and Fieguth, P., "A medical texture local binary pattern for TRUS prostate segmentation", *Proceedings of the 29th International Conference of the IEEE Engineering and Biology Society*, Lyon, France, August 23 – 26, 2007.

[27]. Esgiar, A., Naguib, R., Sharif, B., Bennet, M. and Murray, A., "Fractal analysis in the detection of colonic cancer images", *IEEE Transactions on Information Technology in Biomedicine*, Vol. 6, No. 1, pp 54-58, 2002.

[28]. Press, W., Flannery, B., Teulkolsky, S. and Vetterling, W., "*Numerical recipes in C: the art of scientific computing",* Cambridge University Press, ISBN 0-521-35465-X, UK.

[29]. Julesz, B., "Experiments in the visual perception of texture", *Scientific American*, Vol. 232, pp 34-43, 1975.

[30]. R. C. Gonzalez, R. E. Woods, Digital Image Processing, Pearson Education, 3rd Edition, 2002.

[31]. D. Pham, C. Xu, and J. L. Prince, "Current methods in medical image segmentation", Annu. Rev. Biomed. Eng., Vol. 2, pp. 315-337, 2000.

[32]. Duda, R.O., Hart, R.E., Stork, D.G., *Pattern Classification*. John Wiley & Sons, 2001.

[33]. Vapnik, V. 1995. *The Nature of Statistical Learning Theory*: Springer Verlag.

[34]. R. R. Laddha, S. A. Ladhake, "A Review on Brain Tumor Detection Using Segmentation And Threshold Operations", International Journal of Computer Science and Information Technologies, Vol. 5 (1), 2014, 607-611.

[35]. K. Verma, Aru Mehrotra, Vijayeta Pandey, Shardendu Singh, "Image Processing Techniques for the Enhancement of Brain Tumor Patterns", International Journal of Advanced Research in Electrical, Electronics and Instrumentation Engineering Vol. 2, No. 4, April 2013.

[36]. Ed-Edily Mohd. Azhari, Muhd. Mudzakkir Mohd. Hatta, Zaw Zaw Htike and Shoon Lei Win, "Brain Tumor Detection and Localization in Magnetic Resonance Imaging", International Journal of Information Technology Convergence and Services (IJITCS) Vol.4, No.1, February 2014.

[37]. A. Laxmi, V.Amsaveni and N.Albert, "Detection of Brain Tumor using Neural Network," IEEE transaction, April 2014.

[38]. K. K. Hiran, Ruchi Doshi, "An Artificial Neural Network Approach for Brain Tumor Detection Using Digital Image Segmentation", International Journal of Emerging Trends & Technology in Computer Science (IJETTCS), Vol. 2, No. 5, September – October 2013.

[39]. P. S. Kumar and P. Ganesh Kumar, "Performance Analysis of Brain Tumor Diagnosis Based on Soft Computing Techniques", American Journal of Applied Sciences 11 (2): 329-336, 2014.

[40]. O. N. Pandey, Sandeep Panwar Jogi, Sarika Yadav, Veer Arjun, Vivek Kumar, " Review on Brain Tumor Detection Using Digita l Image Processing", International Journal of Scientific & Engineering Research, Vol. 5, No. 5, May-2014.

[41]. P. John, "Brain Tumor Classification Using Wavelet and Texture Based Neural Network", International Journal of Scientific & Engineering Research, Vol. 3, No. 10, October-2012.

[42]. Magdi B.M Amien, Ahmed Abd-elrehman and Walla Ibrahim, "An Intelligent Model for Automatic Brain Tumor Diagnosis Based on MRI Images" International Journal of Computer Applications(0975-8887) Vol. 72, No. 23, June 2013, pp 21-24.

[43]. D. Assefa, H. Keller, "Multi-Parametric MR Image Processing using Higher Dimensional Vector Algebra", Imaging and Signal Processing in Healthcare and Technology (ISPHT), pp.24 – 31, May, 2011.

Chapter Four

4. NOVEL BRAIN TUMOR DETECTION

4.1 Introduction

The proposed method for detection of brain tumors is based on trinions and trinion based Fourier transforms applied for extracting useful features that could be used to accurately classify tumors and surrounding normal structures. Features derived through this method are inputted to know classifiers and checked for their efficacy. Figure 8 presents the general framework of the proposed method. Before discussing the details of the methodology, some background information on trinions and related subjects as well as the data set used to test the efficacy of the developed scheme shall be presented subsequently below.

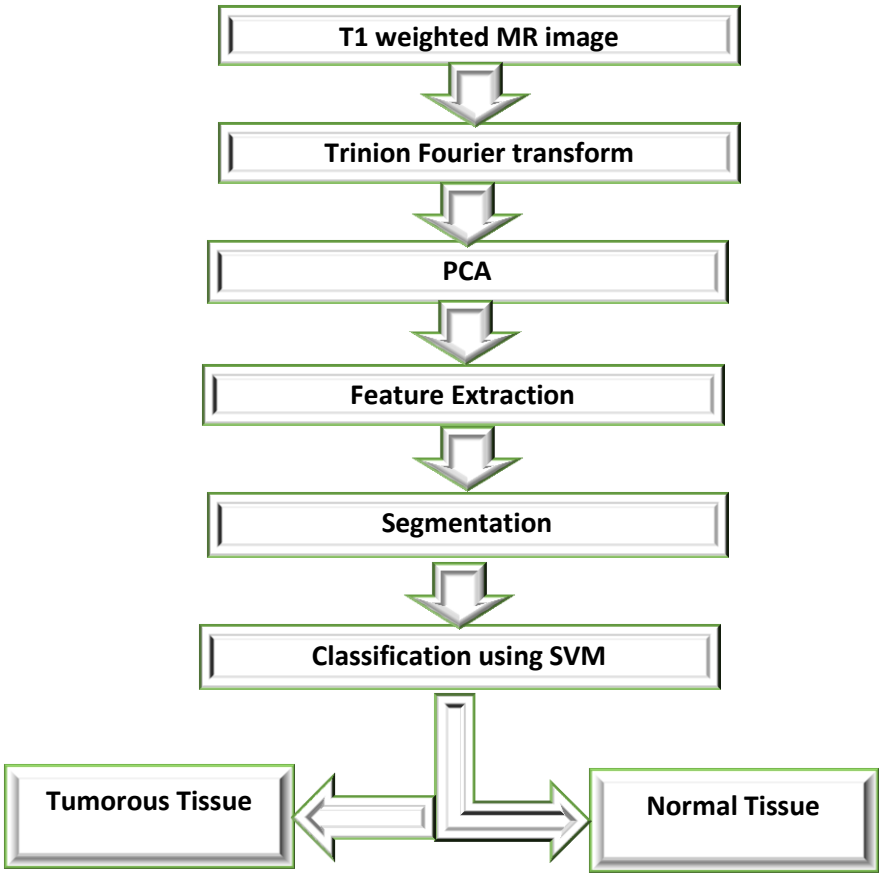

Figure 8: Conceptual framework of the proposed method.

4.2 Data Sets

In this study Gadolinium (Gd) contrast-enhanced T1-W gradient-echo scans of 29 patients treated for the most aggressive form of the gliomas, known by the name Glioblastoma Multiforme (GBM), were used to test the effectiveness of the developed tissue classification and segmentation tool. Both female and male cases as well as different age groups are included in the cohort. GBM is the highest grade (grade 4) and most aggressive of all glioma cases. Previous studies have shown that median survival of patients treated for this kind of cancer is about one year. The T1-W images of the patients were acquired before-, during-, and after-radiation therapy. It is these T1-W images mapped to a trinion with equal real and imaginary components corresponding to the T1-W gray values. Note that a gray scale image can be considered as a special type of color image where the three color components are equal.

All images came with ground truth information based on tumor delineations performed by expert radiologist and those are used as gold standards to compare against the proposed tumor segmentation scheme in this thesis.

4.3 Trinions and Trinion Fourier Transforms

Trinions have one real term and two imaginary components [1]. A trinion number t is defined as:

$$t = a + ib + jc \tag{2}$$

where a, b and c are real numbers, and i, j are operators satisfying the following rules:

$$i^2 = j, \quad ij = ji = -1, \text{ and } \quad j^2 = -i$$

The three base elements $\{1, i, j\}$ of trinions form an abelian (commutative) group where 1 is the unique multiplicative identity element. Distinct from quaternions, trinions with the above structure form a commutative ring. There are other forms of three component numbers proposed in the literature including the ones proposed by Hamilton (while he was developing theory of quaternions). Nevertheless, none of those three component numbers proposed in the earlier attempts have had such a ring structure.

Any trinion number t can be expressed as the sum of a real part and a vector part as:

$$t = s(t) + v(t) \tag{3}$$

where $s(t)=a$ is the real part and $v(t)=ib+jc$ is the vector part.

Any trinion $t = a + ib + jc$ can be written in the form

$$t = |t|(\cos(\phi) + \mu \sin(\phi)) \tag{4}$$

where $|t| = \sqrt{a^2 + b^2 + c^2}$ the amplitude (modulus) is, $\mu = v(t)/|v(t)|$ is the eigen axis, and $\phi = \arctan(|v(t)| / s(t)), 0 \le \phi < \prod$ is the eigen angle (phase). When $|t| = 1$, t is a unit trinion, and when a=0 it is a pure trinion. Details on trinions could be found in [1] and subsequent publications and readers are forwarded to those literatures.

Two working definitions for the trinion Fourier transform (TFT) have been suggested [1]. The TFT of type I is given by:

$$T1(u,v) = \int_{-\infty}^{\infty}\int_{-\infty}^{\infty} h(x,y)(\cos(2\pi(ux+vy)) - \mu_1 \sin(2\pi(ux+vy)))dxdy \tag{5}$$

and its inverse (ITFT) is given by

$$h(x,y) = \int_{-\infty}^{\infty}\int_{-\infty}^{\infty} T1(u,v)(\cos(2\pi(ux+vy)) + \mu_2 \sin(2\pi(ux+vy)))dudv \tag{6}$$

where $h(x, y)$ is generally a trinion valued image function, μ_1 is a unit pure trinion, and μ_2 is a trinion such that the product $\mu_1\mu_2 = -1$. The choice of μ_1 and μ_2 is arbitrary. In [1], $\mu_1 = \frac{(i-j)}{\sqrt{2}}$ and $\mu_2 = \frac{(-1-i+j)}{\sqrt{2}}$ were used.

There exists a type II TFT in the literature [1]. However, many operations of interest including convolutions and correlations are shown to be easier using the type I TFT than type II TFT [1], and hence the former has been adopted in the current study.

The type II TFT and its inverse are computed using the following formulae as proposed in [1].

$$T2(u,v) = \int_{-\infty}^{\infty}\int_{-\infty}^{\infty} h(x,y)(\cos(2\pi ux) - \mu_1 \sin(2\pi ux)(\cos(2\pi vy) - \mu_2 \sin(2\pi vy))dxdy \tag{7}$$

$$h(x,y) = \int_{-\infty}^{\infty}\int_{-\infty}^{\infty} T2(u,v)(\cos(2\pi ux) + \mu_3 \sin(2\pi ux)(\cos(2\pi vy) + \mu_4 \sin(2\pi vy))dudv \tag{8}$$

where μ_1 , μ_2 are unit, pure trinions, and μ_3 , μ_4 are trinions satisfying $\mu_1\mu_3 = -1 = \mu_2\mu_4$. In the above definition the choice of $\mu_1, \mu_2, \mu_3, \mu_4$ is again arbitrary. The simplest choice would be $\mu_1 = \mu_4 = i$ and $\mu_2 = \mu_3 = j$.

The forward-inverse transform relation using both type I and type II TFTs can be verified easily. The trinion based Fourier transforms could be easily discretized using similar discretization principles used in the theory of complex Fourier transforms. The T1-W images are now mapped to the real and the two imaginary components of a trinion as special type of color images and Fourier analysis is executed in the trinion space. It is the intent of the current study to justify the importance of the mapping of the grayscale MR images to a trinion space than the traditional serial way of analyzing such images in the complex space by mapping the images to a real space.

4.4 Principal Component Analysis (PCA)

For the chosen image slices, ROIs were drawn and a voxel-by-voxel analysis was carried out by computing the type I TFT, based on a translating localizing window of size 3 × 3. Following that, vectorial Principal Component Analysis (PCA) [1,2] was applied on each (3 × 3 localized) TFT transformed image, each resulting in a trinion valued output in the new PCA space each of which is a 3 × 3 matrix in our case. This step was needed in order to reduce some redundancy in our multi-channel data. The PCA algorithm used in the current study is the one freely available on the Algorito website at http://algorito.com/algorithm/principal-component-analysis-pca-transform. Now for the purpose of discriminating different tissue structures such as tumors and normal tissues, a metric is calculated for each PCA component. To this purpose, useful texture features which have same form as Haralick features were computed from the PCA transformed matrices.

4.5 Texture Feature Extraction

Ten different ‘Haralick’ features were computed: Sum-average, Sum-entropy, Variance, Energy, Correlation, Homogeneity, Contrast, Entropy, Cluster shade, and Cluster prominence, and tested for their efficacy in uniquely quantifying different objects in our brain MR image data [3]. The features use same formula as Haralick used but obviously computed in a very different way in this study. For example, Gray Level Co-occurrence

Matrix (GLCM) has to computed in order to calculate original Haralick features. In our case, features are computed differently as explained in the previous sub section without the need to compute GLCMs.

$$Energy = \sum_i \sum_j \{p(i,j)\}^2 \tag{9}$$

$$Contrast = \sum_{n=0}^{N_{g-1}} n^2 \Big(\sum_{i=1}^{N_g} \sum_{j=1}^{N_g} p(i,j)\Big), |i-j| = n \tag{10}$$

$$Correlation = \frac{\sum_i \sum_j ij\,(p(i,j)) - \mu_x \mu_y}{\sigma_x \sigma_y} \tag{11}$$

$$Variance = \sum_i \sum_j (i-\mu) p(i,j), \quad \mu \text{ is mean of } p(i,j) \tag{12}$$

$$\text{Inverse Difference Moment} = \sum_i \sum_j \frac{1}{1+(i-j)^2} p(i,j) \tag{13}$$

$$Entropy = -\sum_i \sum_j p(i,j) \log(p(i,j)) \tag{14}$$

$$\text{Sum Average} = \sum_{k=2}^{2N_g} i p_{x+y}(k) \tag{15}$$

$$\text{Sum Entropy} = -\sum_{k=2}^{2N_g} p_{x+y}(k) \log\{p_{x+y}(k)\} \tag{16}$$

$$\text{Cluster Shade} = \sum_i \sum_j \{i + j - \mu_x - \mu_y\}^3 * p(i,j) \tag{17}$$

$$\text{Cluster Prominent} = \sum_i \sum_j \{i + j - \mu_x - \mu_y\}^4 * p(i,j) \tag{18}$$

where $P(i,j)$ represents (i,j)'th entry in a normalized gray-tone spatial dependence matrix, $p(i)$ represents i'th entry in the marginal-probability matrix obtained by summing the rows of $p(i,j)$,

$$p(i) = \sum_{j=1}^{N_g} p(i,j) \tag{19}$$

N_g - represents number of distinct gray levels in the quantized image.

$\sum_i$ and $\sum_j$ Represent $\sum_{i=1}^{N_g}$ and $\sum_{j=1}^{N_g}$, respectively,

$$p_{x+y}(k) = \sum_{i=1}^{N_g} \sum_{j=1}^{N_g} p(i, j), \; k=i+j \tag{20}$$

$$\mu_x = \sum_{i=1}^{N_g} ip(i, j) \;\; And \;\; \mu_y = \sum_{j=1}^{N_g} jp(i, j) \tag{21}$$

$$\sigma_x{}^2 = \sum_{i=1}^{N_g} (p(i) - \mu_x)^2 \;\; And \;\; \sigma_y{}^2 = \sum_{j=1}^{N_g} (p(j) - \mu_y)^2 \tag{22}$$

In our case $N_g = 3$.

4.6 Support Vector Machine (SVM) based Classification

In the case of linear separable data, the linear Support Vector Machine (SVM) classifier tries to find among all hyperplanes that minimize the training error, the one that separates the training data with maximum distance from their closest points (maximal margin hyperplane).

$$F(x) = \sum_{i \in S} a_i Y_i K(x_i, x) + b \tag{23}$$

where x is the feature vector to be classified, i indexes the training sample, α_i are Lagrange multipliers, S is a set of indices for which x_i is a support vector, i.e., a vector for which $\alpha_i \neq 0$ after optimization, a_i and b (bias) are fitted to the data to maximize the margin, Y_i is the label [-1, 1] of training sample i, and K is the kernel function [4]. A serious problem with nonlinear kernel SVMs is their complexities of classification which are high when a large number of support vectors are needed [5]. There are many kernels that can be used, such as linear, polynomial, radial basis function (RBF) and sigmoid.

In this study a linear kernel and a regularization parameter $C=1$ have been used. The support vectors, a_i and b were all automatically obtained by the SVM training procedure. The performance of the selected SVM classifier was then quantified based on its sensitivity, specificity and the overall accuracy on the test (training) samples, which in our case are based on the normal and abnormal (cancerous) tissues of the brain scans of the GBM patients under consideration.

Reference

[1]. D. Assefa, L. Mansinha, K. F. Tiampo, H. Rasmussen, and K. Abdella, The trinion Fourier transform of color images, Signal Processing, 91(8), pp. 1887-1900, 2011.

[2]. H. Witjes, M. Rijpkema, M. van der Graaf, W. Melssen, A. Heerschap & L. Buydens, Multispectral Magnetic Resonance Image Analysis Using Principal Component and Linear Discriminant Analysis. Technical Note, *Magn. Reson. Imaging*, Vol. 17, 2003, 261-269.

[3]. Haralick, R.M.; Shanmugam K. & Dinstein, I. Texture features for image classification. *IEEE Transactions on Pattern Analysis and Machine Intelligence*, Vol. SMC-3, No. 6, Nov 1973, 610-621.

[4]. A. Osareh, Comparative exudate classification using support vector machines and neural networks, Proc. Int. Conf. Medical Image Computing and Computer-Assisted Intervention-Part II, Springer, Verlag, London, UK, pp. 413-420, 2002.

[5]. Aparna M. Nichat and S. A. Ladhake, Brain Tumor Segmentation and Classification Using Modified FCM and SVM Classifier, IJARCCE, Vol. 5, No. 4, April 2016.

Chapter Five

5. RERSULTS AND DISCUSSION

5.1 Feature Map Selection for Segmentation of Brain Tumor

Based on a comparison against the available ground truth, generated feature (signature) maps were assessed for their efficacy in uniquely detecting tumorous regions on all the T1-W MR images included in the data sets considered in this thesis. The best selected feature is subsequently used for automated segmentation and classification of the cancerous and normal tissues. Note that the feature selection was done by qualitative means simply by comparing the area enclosed by color cancerous signatures offered by the features against the manual delineations by the radiologist. Those features with promising performance are then checked for their efficacy in effective classification of cancerous and normal (non-cancerous) tissues. For the pixel based classification experiment, 1000 tumorous pixels and 2000 normal pixels were manually selected to analyze the class separability of tumorous and normal pixels. For each image, the tumor training set is made up by pixels belonging to small isolated tumors. Their characteristics can represent the rest of tumors in the image. Additionally, 146 normal and 65 tumorous images were used to train the classifier for performing image based brain tissue classification. Again, these images are assumed representatives of the rest of the images in the dataset.

5.2 Signature Map Results

Signature maps generated using cluster prominence feature generally showed superior performance in detecting cancer tissues as confirmed by the available ground truth which is tumor delineations by an expert radiologist. The signature map correctly differentiated tumorous tissue from normal brain tissue. Figures 6 and 7 present signature map results generated using the cluster prominence feature for selected T1-W MR slices of different patients. The cyan color on the signature maps depicts the tumor area while the white lines were delineations from the radiologist. As could be seen on the figure, there is a good match between tumor signatures generated automatically using the proposed algorithm and the radiologist’s contour. The

examples presented showed both uni-focal (Figure 9) and multi-focal (Figure 10) brain tumor cases. There are at least two visible issues on the signature map. One is the overlap of tumor signatures with the skull boundary. That is not considered a serious issue in the current study. Most often, whenever such automated schemes are developed for tumor detection and segmentation, the brain tissue is segmented out and the algorithm is applied on the brain only. The brain and the skull boundary should not be processed at the same time. So we should simply omit/ignore the skull boundary signatures seen on the signature map. The other issue is areas around the eye. This is a similar issue like the skull and should be omitted from the analysis.

Looking at the results, it is obvious that the proposed algorithm slightly under estimates the tumor area when compared with the radiologist's contour. A further observer study (comprising of more than one expert radiologist) could alter the results while such subject is beyond the scope of the current study. But in general, it could be said that there is a very good much between the signature maps showing the brain tumors and that of the radiologist's contour.

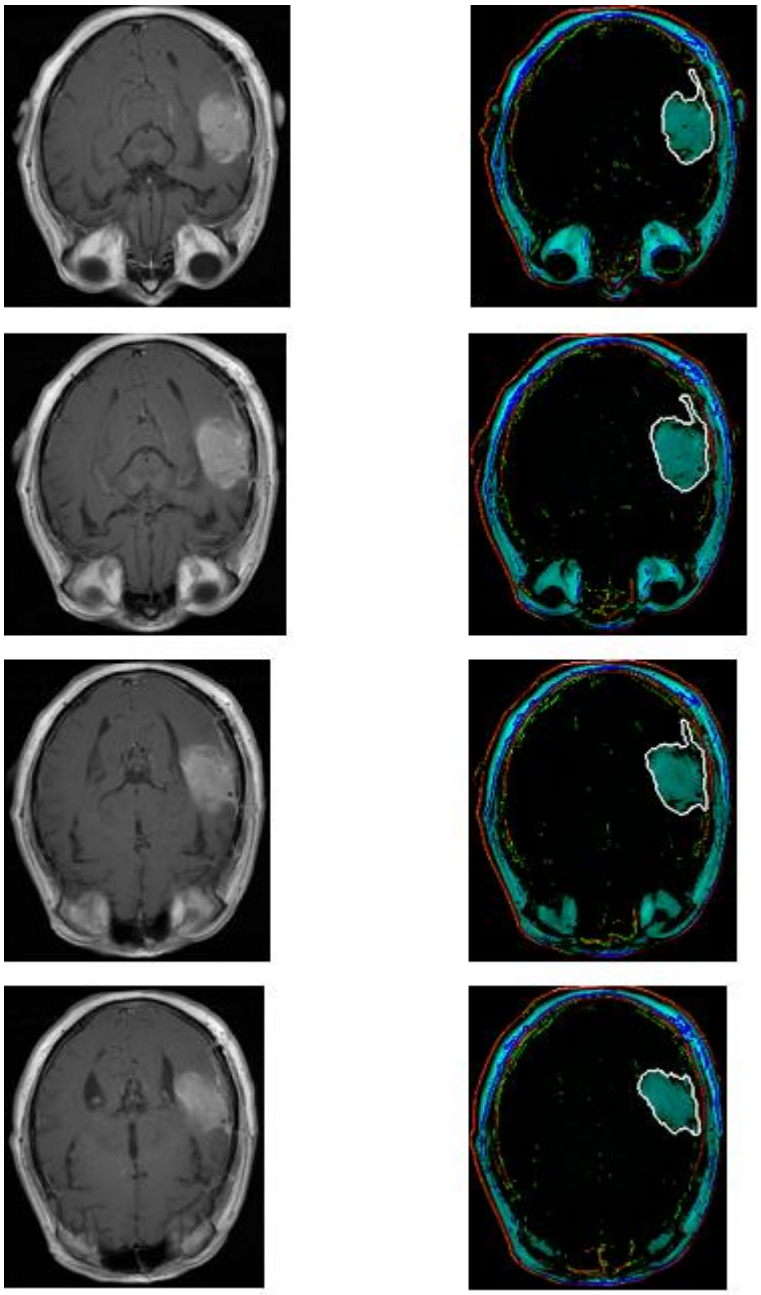

Figure 9: Brain tumor detection results: original T1-W MR image (1st column) and the respective signature maps generated using the proposed scheme (2nd column). White lines are delineations from the radiologist used as the gold standard.

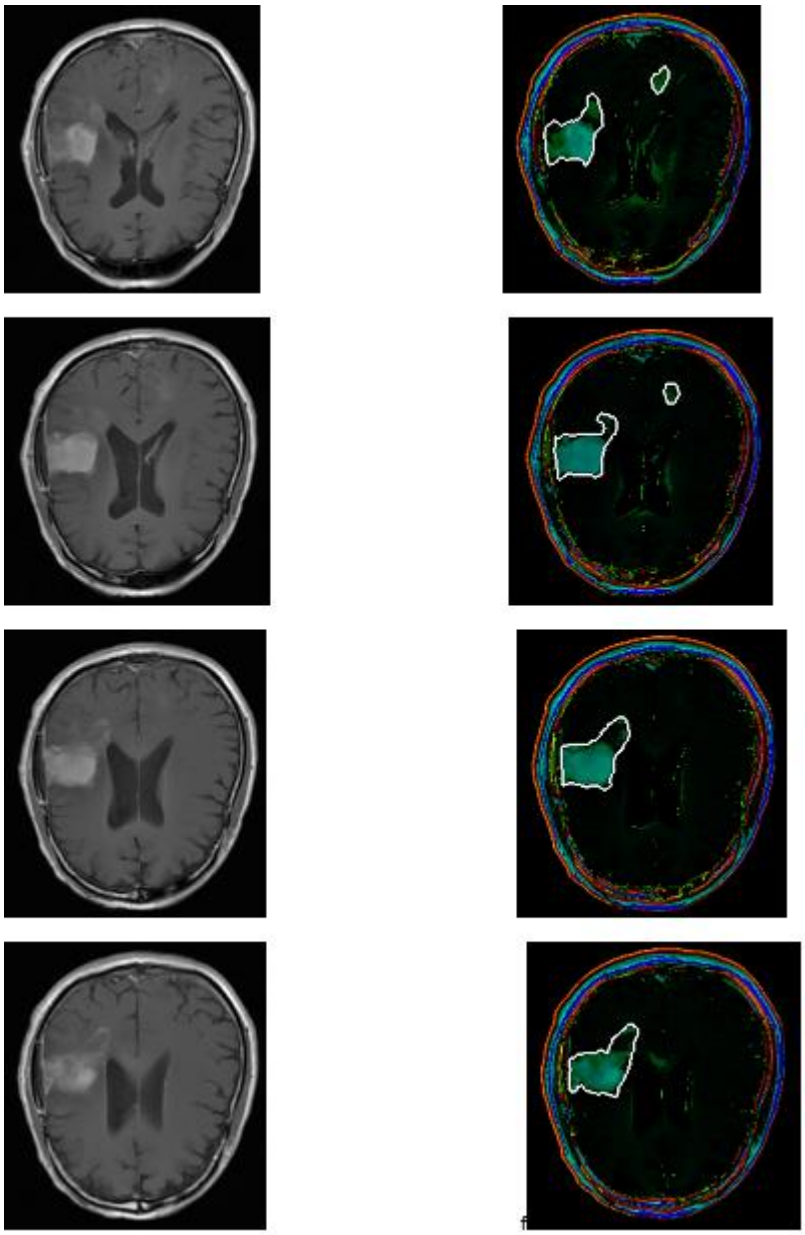

Figure 10: Brain tumor detection results: original T1-W MR image (1st column) and the respective signature maps generated using the proposed scheme (2nd column). White lines are delineations from the radiologist used as the gold standard.

5.3 Segmentation

Segmentation has been performed on 211 MR images. This was done by making use of SVM to classify the brain tissue into tumorous and healthy. The green and blue intensities of the signature maps were inputted to the SVM omitting the red component. Through experiment, it was found that the red component of the signature maps was of little use for differentiating tumorous and normal tissue pixels while the green and blue components were of great use. The SVM was trained and tested that

way. Figure 11 depicts typical (binary) segmentation results generated where white signifies tumor while the rest of the back ground was labeled black. Same comments as before apply regarding the skull boundaries and regions around the eyes.

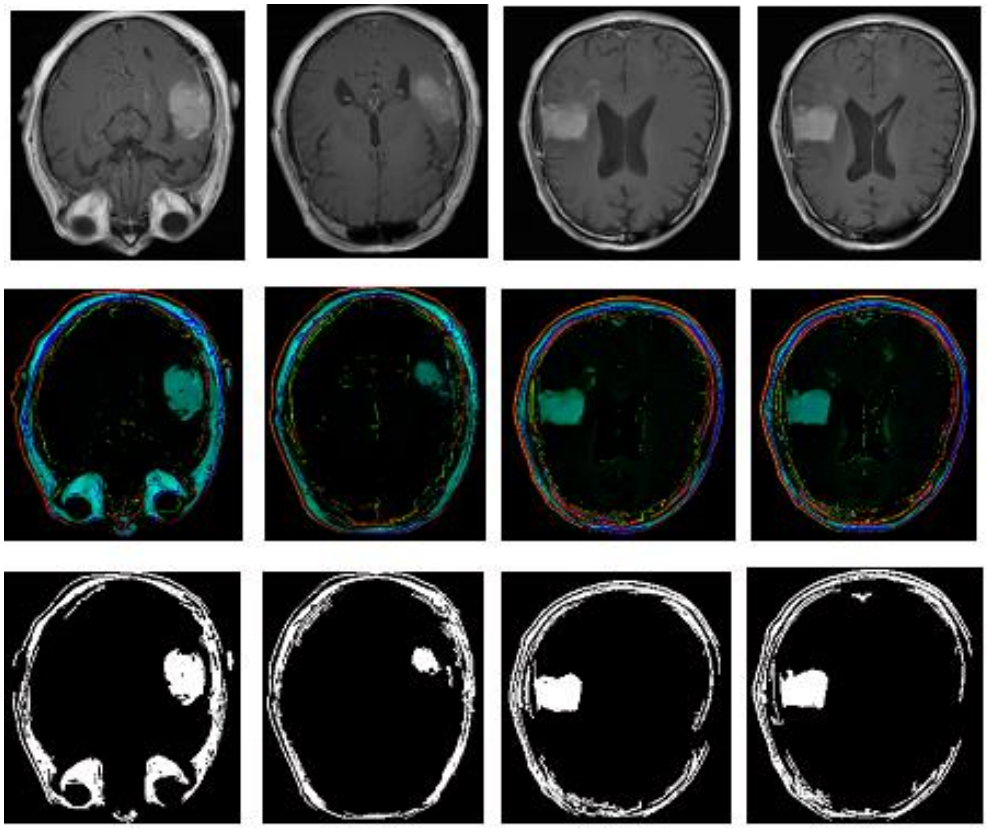

Figure 11: Brain tumor detection results: original T1-W MR images (1st row), the respective signature maps generated using the proposed scheme (2nd row), and respective segmented images (3rd row).

5.4 Performance Evaluation of the Proposed Method

In this thesis the accuracy of the proposed brain tumor detection algorithm is evaluated by deriving quantitative measures comparing each segmented MR image mask with the available ground truth/gold standard. The SVM was trained and tested using features derived from the signature maps as explained in the previous section. Two different criteria were set up in this regard: pixel-based criteria and image-based criteria. The first criterion examines the ability of the proposed algorithm for pixel base detection (i.e. segmentation) of brain tumor while the second one evaluates algorithm's ability to distinguish (i.e. classify) between images being tumorous and non-tumorous. In the case of the pixel based criteria, 2100 tumorous pixels and 3200 non tumorous pixels

were taken from 211 brain MR images. While for the image based criteria, 146 tumor free and 65 images with certain manifestations of a tumor were considered.

Classification performance is evaluated based on three matrices: sensitivity, specificity and overall accuracy. The confusion matrix used to compute the accuracy measures is defined in terms of the combination of number of true positives (TP), number of true negatives (TN), number of false positives (FP) and number of false negatives (FN), which are computed by comparing the algorithm's output with that of the gold standard (see Table 1).

Expected outcome	Ground truth		Row total
	Positive	Negative	
Positive	TP	FP	TP+FP
Negative	FN	TN	FN+TN
Column Total	TP+FN	FP+TN	TP+FN+ FP+TN

Table 1: Confusion matrix defining the terms TP, TN, FP, and FN.

TP indicates the total number of abnormal (cancerous) cases correctly classified, TN indicates the number of normal cases correctly classified, FP signifies number of wrongly detected/classified abnormal cases when they are actually normal cases and FN indicates the number of wrongly classified normal cases when they are actually abnormal cases [1].

The quality rate parameter accuracy is the proportion of total correctly classified cases i.e. abnormal classified as abnormal and normal classified as normal from the total number of cases examined [1-4]. Table 2 shows the formulas to calculate accuracy, sensitivity, and specificity metrices.

Quality parameters	Formulas
Sensitivity	$\frac{TP}{TP + FN}$
Specificity	$\frac{TN}{TN + FP}$
Accuracy	$\frac{TP + TN}{TP + TN + FN + FP}$

Table 2: Accuracy, sensitivity and specificity calculations.

Table 3 summarizes the computed accuracy measures for image based classification. Accordingly, the proposed scheme offered a minimum overall accuracy of around 83% and a maximum accuracy of 95% with an average of around 91% showing commendable outcomes. The average sensitivity was 91% while the average specificity was around 90%.

Patient	Ground Truth		Slice classification using proposed method						
	Tumorous (T)	Normal (N)	TP	TN	FP	FN	Sensitivity	Specificity	Accuracy
Patient 3	12	28	10	26	2	2	0.83	0.93	0.90
Patient 9	10	29	10	27	2	0	1	0.93	0.95
Patient 18	8	14	7	13	1	1	0.88	0.93	0.91
Patient 21	9	32	9	29	3	0	1	0.91	0.93
Patient 23	11	23	10	21	2	1	0.91	0.91	0.91
Patient 24	15	20	13	16	4	2	0.87	0.8	0.83
Patient 26	11	13	10	12	1	1	0.91	0.92	0.92
Total	65	146	59	132	14	6	0.91	0.9	0.91

Table 3: Tumorous slice classification results.

A similar performance measure was carried out for the pixel based classification. Figures 12 and 13 show the classification results. Both the training as well as the testing results are presented.

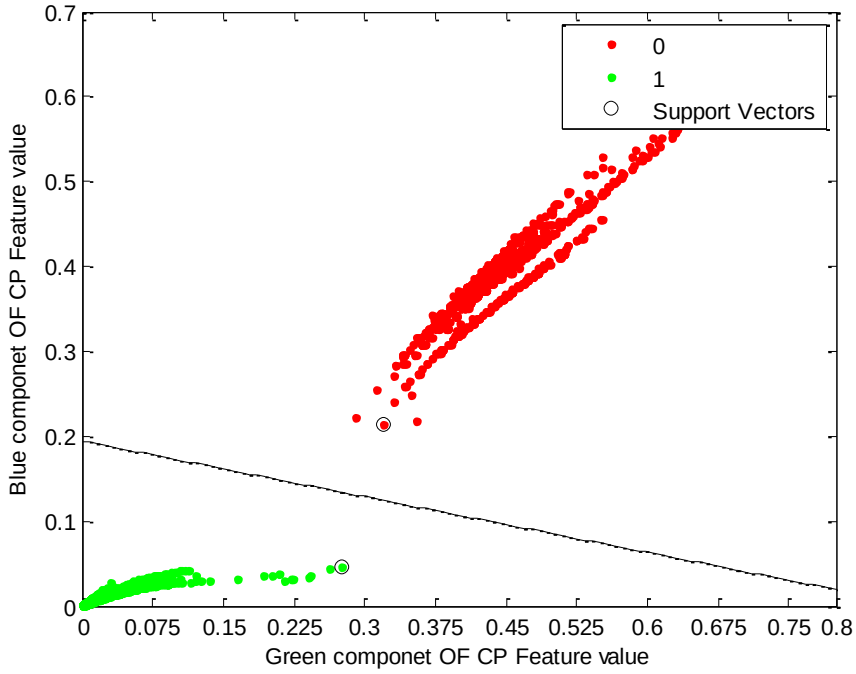

Figure 12: SVM training of pixel.

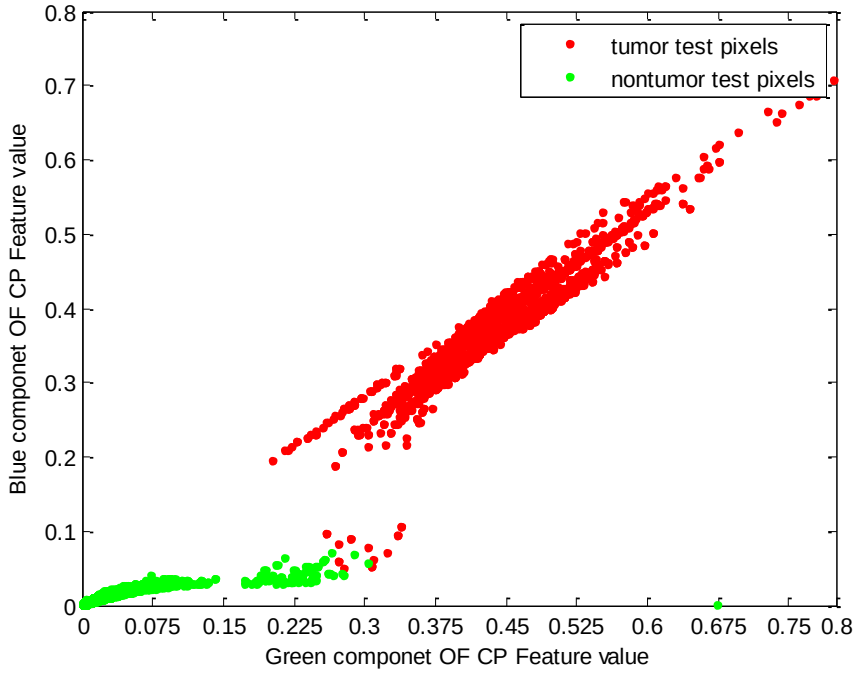

Figure 13: Test for tumorous and non-tumorous pixels.

The training was done for 1000 green and blue components of the tumorous pixel as depicted on the generated signature maps and 2000 green and blue components of the normal pixels taken. In this case the algorithm showed a remarkable performance offering 99.8% accuracy, 99.6% sensitivity and 100% specificity.

5.5 Discussion

As demonstrated in the previous section, the performance of the proposed classification and segmentation scheme is promising in most cases. The scheme detected and segmented the brain tumors with an acceptable accuracy when compared with the physician's contour. What we need to notice is that the manual contour comes with some challenges. One is it is prone to observer variability. Also it is not repetitive and often time consuming procedure. The automation could circumvent such issues considerably and could greatly enhance the manual delineation procedure. The computed sensitivity, specificity as well as overall accuracy measures were commendable.

There are however certain cases which are challenging and affecting the performance of the proposed algorithm. Such cases include cystic tumors, necrotic structures and the like. Such subjects appear very dark when seen on the contrast enhances T1-W images. The algorithm has difficulties taking such objects as tumors. Note that it is possible a cyst may or may not be cancerous. In our case, all cases considered were those with confirmed grade 4 (highest grade) glioma cancers known by the name glioblastoma multiforme (GBM). An example is presented in Figure 14 to demonstrate the scenario. In such cases the cancer signatures generated by the proposed methodology show significant deviations from those contoured manually. More investigations and clinical validations might be requires to further evaluate the performance. It might also be needed to perform an observer study to check how sensitive the proposed algorithm is to different ground truth/gold standard information coming from more than one oncologist.

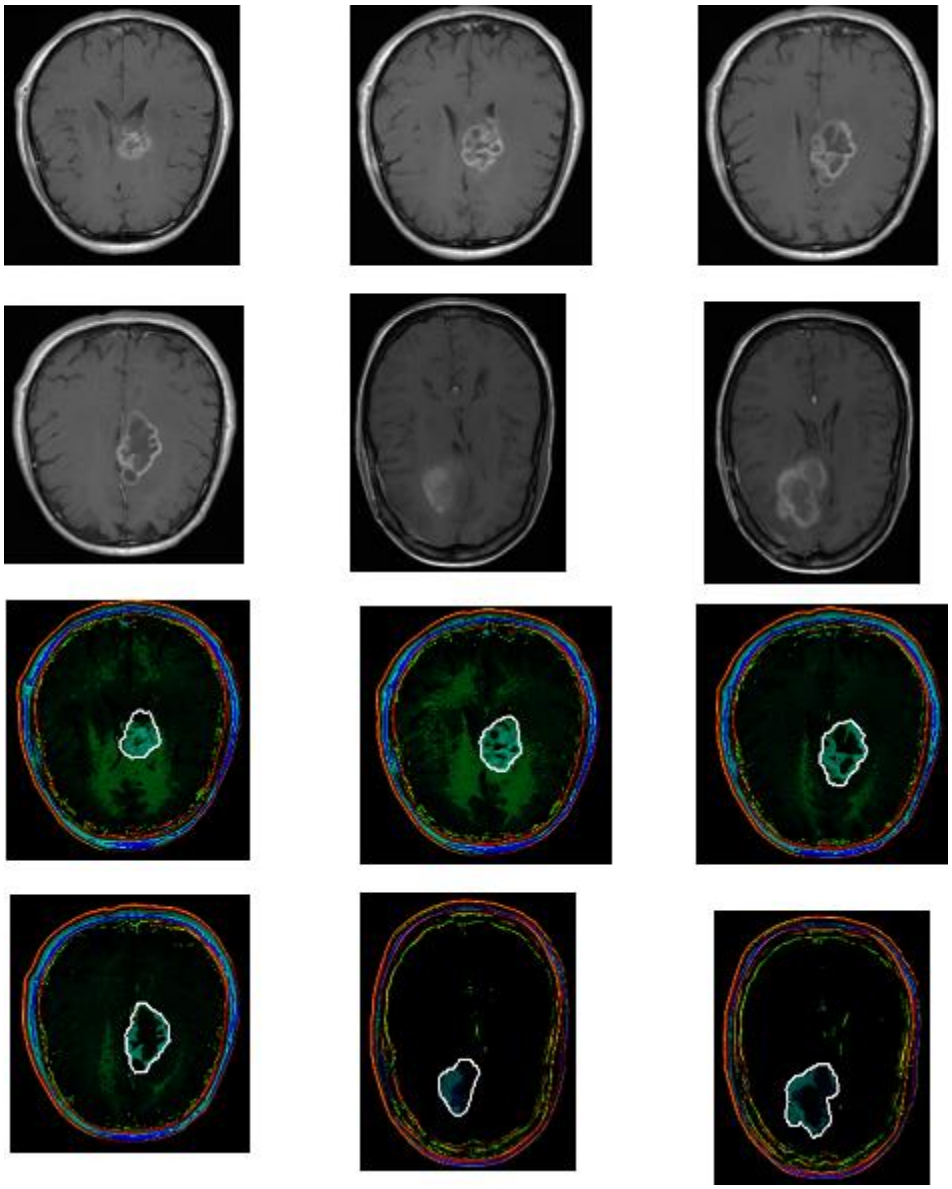

Figure 14: Signature map results for patients with cancerous tissues composed of dark objects (eg. cyst, necrotic structures etc). White lines are delineations from the radiologist used as the gold standard: Original T1-W MR images (1st and 2nd row) and the respective signature maps generated using the proposed scheme (3rd and 4th row).

Reference

[1]. Provost, F., Fawcett, T., 1997. Analysis and visualization of classifier performance: Comparison under imprecise class and cost distributions. In: Proc. Third Internat. Conf. on Knowledge Discovery and Data Mining (KDD-97). AAAI Press, Menlo Park, CA, pp. 43–48.

[2]. Lane, T., 2000. Extensions of ROC analysis to multi-class domains. In: Dietterich, T., Margineantu, D., Provost, F., Turney, P. (Eds.), ICML- 2000 Workshop on Cost-Sensitive Learning.

[3]. Egan, J.P., 1975. Signal detection theory and ROC analysis, Series in Cognition and Perception. Academic Press, New York.

[4]. Hand, D.J., Till, R.J., 2001. A simple generalization of the area under the ROC curve to multiple class classification problems. Mach. Learning 45 (2), 171–186.

Chapter Six

6. CONCLUSION AND FUTURE WORK

6.1 Conclusion

For use in T1-W MR image analysis, the approach proposed in this thesis, which combines trinions, their Fourier transforms and Principal Component Analysis (PCA), allowed to extract useful higher order features to detect and segment objects of interest. The scheme has been applied in uniquely detecting and segmenting GBM tumors, the highest grade and aggressive form of brain tumor. The color signature maps generated using the computed features were able to identify useful objects not obvious on the original gray scale T1-W images. One of the features, namely cluster prominence, particularly offered the best results. Performance of the proposed scheme has been checked against available ground truth information and has been found to be promising. Both uni-focal and multi-focal tumor cases have been considered. Cases with cystic tumors and necrotic structures are considered difficult for the proposed algorithm.

6.2 Future work

A way to segment the brain omitting the skull boundary as well as regions around the eye could enhance the performance of the algorithm. It would also be interesting to check the performance of the proposed scheme on other non GBM brain tumor cases. Other than use of SVM during the classification stage, use of other classifiers including an Artificial Neural Network (ANN) could be interesting to look at. The clinical evaluation of the scheme is subject to much further investigation. Such features similar to the ones used in this thesis to segment GBM tumors are believed to have great potentials in quantification of patient responses (Eg. disease progression). Such and similar other issues however require much further researches to be carried out.

Reference

[1]. Galloway, M.M. (1975). Texture analysis using grey-level run lengths. Computer Graphics and Image Processing, Vol. 4, pp. 172-179.

[2]. Kadam D. B., Gade S. S., M. D. Uplaneand R. K. Prasad, ―Neural Network Based Brain Tumor Detection Using MR Images, *International Journal of Computer Science and Communication (IJCSC)*, Vol. 2, No. 2, July-Dec. 2011, pp. 325-331.

[3]. Nikola K. Kasabov, *Foundations of Neural Networks, Fuzzy Systems, and Knowledge Engineering*, Massachusetts Institute of Technology, 1998, pp. 167-473

[4]. Louis D.N., Ohgaki H., Wiestler O.D, Cavenee W.K. (Eds.), ―WHO Classification of Tumors of the Central Nervous System, *International Agency for Research on Cancer (IARC)*, Lyon, France, 2007.